# 5. Sensitivity of crustal velocities in Fennoscandia to radial and lateral viscosity variations in the mantle


## Abstract[a]

We investigate the sensitivity kernels of the present-day velocities in Fennoscandia induced by the retreat of the Late Pleistocene ice sheets with a 3D Finite-element model having compressible, viscoelastic material properties and a realistic ice load history of the Fennoscandian ice sheet. The model is subdivided into blocks of variable size, which results in a large number of kernels to interpret. Thus, we introduce a simple approach to calculate the kernel of a block by averaging the perturbed predictions of all surface nodes of this block to one value for this block.

Our results show that the present-day uplift velocity is mostly sensitive to upper-mantle layers between 220 and 540 km depth, independent of the block size. Velocities in blocks located inside the former ice sheet area are more sensitive to viscosity variations than velocities in blocks located outside the former ice sheet. The largest effects are found for blocks located below the former ice maximum on the surface. The uplift velocity in smaller blocks is more sensitive to viscosity changes than in larger blocks.

For the present-day horizontal velocity, the sensitivity depends on the block size and the location of this block in relation to the former ice sheet. In general, lateral viscosity variations in the transition zone of the mantle have a strong influence on the tangential motion. A comparison of the results of smaller and larger blocks also indicates higher sensitivities for the horizontal velocities of larger blocks.


[a] Steffen, Wu and Kaufmann (2006b). Sensitivity of crustal velocities in Fennoscandia to radial and lateral viscosity variations in the mantle, Earth Planet. Sci. Lett., submitted.

## 5.1 Introduction

The viscosity of the mantle is a very important parameter in the study of geodynamics and the evolution of the Earth. Observations of the glacial isostatic adjustment (GIA) process such as palaeo-shorelines and global positioning system (GPS) measurements can be used to constrain the material properties of the Earth, especially the mantle viscosity. As mantle viscosity can vary in all three dimensions, the observations are equally sensitive to radial and lateral changes of this parameter. This means that if one varies the viscosity in a certain depth or region of the mantle, a measure of the sensitivity of a certain datum can be provided. Wu [2006] has presented such an approach for observations of relative sea levels and crustal velocities in North America using an axisymmetric, laterally heterogeneous, self-gravitating

spherical viscoelastic earth model. For an earth model with a laterally variable viscosity he showed that if there is only one perturbed region, its influence is usually strongest for the sites lying directly above. With increasing depth, the width of its influence increases also to neighboring regions, but with decreasing signal level. In contrast, the closer the region lies to the ice load the stronger the signal level. In general, data from any location are most sensitive to viscosity variations in regions below the former ice load, e. g. if there is more than one perturbed region, the influence from the region near or below the ice load dominates the influence. He also found a trade-off between radial and lateral viscosity variations, which complicates the inversion of mantle viscosity. Another interesting result is that regions with viscosity variations lying underneath the ice sheet can influence tangential velocities at sites far away from the former ice sheet. However, these results are obtained with an axisymmetric and simple ice model, which allows the tangential velocity to be calculated only in direction normal to the ice sheet margin. Therefore one of the aims of this paper is to investigate the sensitivity kernel without the assumption of axisymmetry and with a *realistic* ice model.

These so called sensitivity or Frech´et kernels can be very useful for finding the optimal location of sites that are most sensitive to the viscosity variation in a certain region. Since Peltier [1976], a number of works used sensitivity kernels [e. g. Mitrovica and Peltier, 1991, 1993, 1995; Peltier and Jiang, 1996a,b; Peltier, 1998; Milne et al., 2004; Wu, 2006]. For example, Mitrovica and Peltier [1991] investigated the radial dependence of the kernels. Milne et al. [2004] calculated sensitivity kernels of the radial and tangential velocities for 8 BIFROST GPS stations to determine the resolving power of the BIFROST data set. Except for one station (Hässleholm) they found "moderate, but a nonnegligible sensitivity to variations in lower-mantle viscosity (at least in the shallowest portions of this region)". The sensitivity of the horizontal velocities is largest in the uppermost mantle (sub-lithosphere to 450 km), but nonzero near the base of the mantle at some sites. Furthermore, the sensitivity of the uplift velocity receives large contributions by upper-mantle viscosity changes, but the upper lower-mantle also influences these contributions. In contrast, Steffen et al. [2006a] showed with a flat three-dimensional (3D) earth model that the uplift velocity is not strongly influenced by the lower mantle and the horizontal velocities receive large contributions from 3D viscosity variations in the transition zone of the upper mantle between 450 and 660 km depth. This difference in the results of both papers might be explained by the possibility that the sensitivity seen by the global model of Milne et al. [2004] is actually from GIA contribution from the Laurentide ice sheet [Wu, 2006]. However, the difference in sensitivity for horizontal velocities still needs to be explained. Thus, another aim of this paper is to clarify the different results of Milne et al. [2004] and Steffen et al. [2006a].

It has been shown earlier that for GIA predictions in the Scandinavian region the flat-earth approach is adequate [e.g. Wolf, 1984; Amelung and Wolf, 1994; Wu and Johnston, 1998]. It was successfully used in the last decade [e. g. Wu et al., 1998; Kaufmann and Wu, 1998a,b; Kaufmann et al., 2000; Kaufmann and Wu, 2002; Kaufmann et al., 2005; Wu, 2005; Steffen et al., 2006a], and complements newer results based on 3D spherical earth models [e. g. Wu, 2002; Wu and van der Wal, 2003; Zhong et al., 2003; Wu et al., 2005; Latychev et al., 2005b; Wang and Wu, 2006a,b,c; Spada et al., 2006]. A main result of these papers is that a realistic 3D variation in mantle viscosity produces significantly different model predictions than a simpler 1D mantle-viscosity model. In addition, the investigations by Steffen et al. [2006a] showed that the lower mantle itself as well as a possible 3D viscosity structure of the lower mantle beneath Fennoscandia have no significant influence on the velocities and sea-level observations in that region.

To summarise, this paper will deal with the following: we focus on data in Fennoscandia since a large set of different observations, both in space and time, are available. But, in contrast to the work of Wu [2006]

related to the Laurentide ice sheet, who used an axially symmetric earth model with a simple symmetric ice model, (i) we apply a *realistic* ice load history of the Fennoscandian ice sheet - namely the RSES ice model from Kurt Lambeck - on the model surface and (ii) we employ a *flat* 3D FE model with compressible, viscoelastic material properties. We have chosen this model approach as it is simple, efficient in computation time and memory requirements, and, in comparison to spherical investigations, the smaller distribution of regions with viscosity variations might provide more precise information concerning the sensitivity of the Earth's 3D structure. This allows us to explore the sensitivity of different data from different parts of Fennoscandia with a realistic ice history.

Our main emphasis is to show how sensitive BIFROST stations are to special mantle layers and regions and to suggest ideal locations for new GPS stations with higher sensitivity.

## 5.2 FE-Modelling

### 5.2.1 Earth models

The GIA process in Fennoscandia is modelled using the finite-element (FE) method. A changing ice load is applied to the surface in a central region of 3000 km $\times$ 3000 km of a flat, viscoelastic earth model which is described in Steffen et al. [2006a]. The horizontal element size is 100 km, which results in 900 element surfaces and 961 nodes. It is a layered, isotropic, compressible, Maxwell-viscoelastic half-space with a constant gravitational attraction of $g = 9.82$ m s$^{-2}$. We solve the Boussinesq problem for a layered, viscoelastic half-space using the commercial finite-element package ABAQUS, which has been modified to include pre-stress in order to allow the deformed free surface to return to its initial equilibrium via viscous flow [see Wu, 2004, for a summary]. The validity of the finite-element model to predict glacial isostatic adjustment has been shown previously [Wu and Johnston, 1998]. To allow the mantle material to flow due to application of a surface load outside the area of interest, we follow the approach described in Steffen et al. [2006a] and enlarge the model in horizontal direction with a peripheral frame of 60,000 km width.

Generally, our earth models consist of a layered elastic lithosphere over a layered viscoelastic mantle [see Steffen et al., 2006a, for more information]. All models have a uniform 70-km-thick lithosphere. The upper as well as the lower mantle are divided in to 4 layers, respectively. Density $\rho$, shear modulus $\mu$ and bulk modulus $\kappa$ are volume-averaged values derived from PREM [Dziewonski and Anderson, 1981], and they are considered to be constant within an element. The 1D viscosity profile used for the sensitivity analysis is the viscosity profile V1 from Steffen et al. [2006a], characterised by only two different viscosity values, an upper-mantle viscosity of $4 \times 10^{20}$ Pa s and a lower-mantle viscosity of $2 \times 10^{22}$ Pa s. This parameterisation has been derived from fitting GIA observations of the Scandinavian region and has been confirmed by several independent studies [e.g. Lambeck et al., 1998a; Wieczerkowski et al., 1999; Milne et al., 2001; Kaufmann and Wu, 2002; Milne et al., 2004; Steffen and Kaufmann, 2005].

One of the challenges we face in studying the sensitivity kernel for a 3D problem is the very large number of model calculations - each with viscosity perturbation in a certain block in the 3D earth model. To overcome this challenge, we adopted the following strategy: First, we consider a small number of blocks, then we progress with more but smaller blocks. For each case, the models are termed UM$i$_B$j$, where UM$i$ with $i \in [1,4]$ refers to one of the upper-mantle layers and B$j$ is the block number. Every model represents a laterally homogeneous model except one block of one layer having a half an order of magnitude higher viscosity of $1.26 \times 10^{21}$ Pa s [as suggested by Wu, 2006]. This approach is used

due to the results of Steffen et al. [2006a] only for the upper mantle of the model. They found that the observed GIA process in Fennoscandia (i) is not very sensitive to the viscosity structure in the lower mantle and (ii) to the lower mantle itself. We employ three different models with varying resolution:

1. Coarse model:
   At first, the central frame is subdivided into 4 central blocks of 1000 km $\times$ 1000 km, respectively, and a frame of 500 km width (Fig. 5.1a). The viscosity is changed in only one of the blocks and in only one of the four upper-mantle layers. Hence, we have 16 different models (4 layers $\times$ 4 blocks). This division allows us to investigate in a simple way the sensitivity kernel of the central Fennoscandian region below the ice sheet and the horizontal size of 1000 km is comparable to the smallest grid of 7.5° ($\sim$ 835 km) of Wu [2006]. In addition, the quite perfect arrangement of the 4 blocks around the uplift centre in the Gulf of Bothnia eases the discussion of the horizontal velocities. Every block consists of 100 elements and has 121 nodes on the surface.

2. Intermediate model:
   Next, we subdivide the whole central area into 9 blocks of 1000 km $\times$ 1000 km, respectively (Fig. 5.1b). This division with models of the same block size allows a discussion of the sensitivity

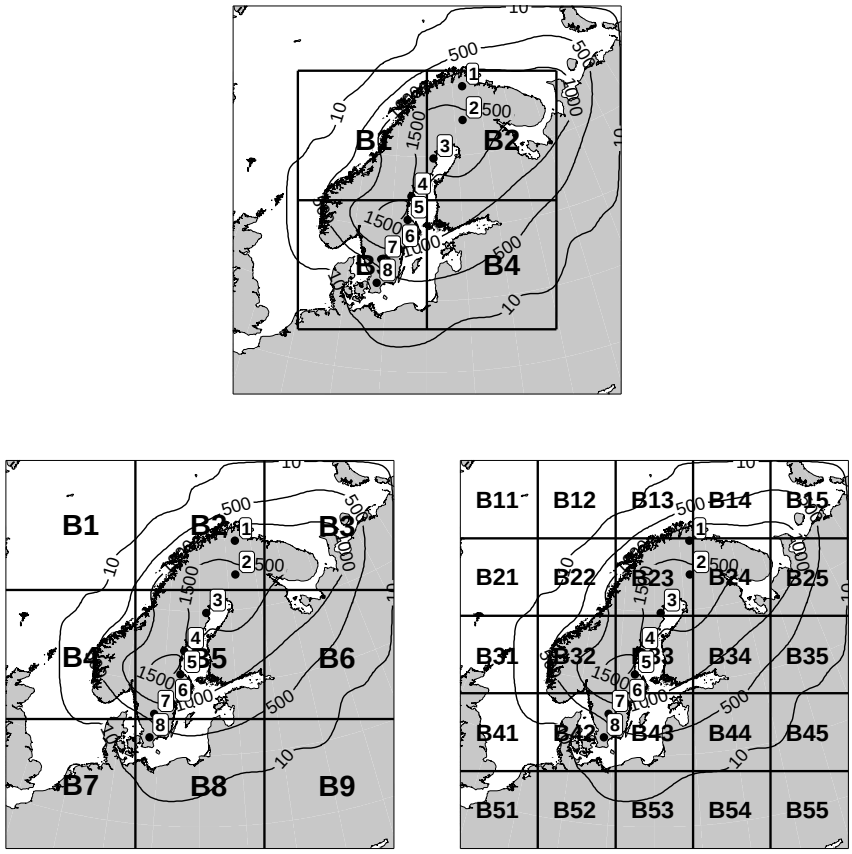


Figure 5.1: Finite-element block structure over Fennoscandia. The ice sheet thickness (in m) at 22,000 years BP is drawn with contours. Dots mark the 8 selected BIFROST locations of Figs. 5.8 - 5.10. From north to south: Kevo (1), Sodankyla (2), Skelletea (3), Sundsvall (4), Martsbo (5), Norrkoping (6), Jonkoping (7) and Hässleholm (8).

kernels of the whole Fennoscandian region. Furthermore, block B5 is located in the central uplift region, which allows a discussion of the velocities' direction in comparison to the position of the former ice load. Changing the viscosity in only one of the blocks and only one of the layers, we have 36 different models for our investigation. Again, every block consists of 100 elements and has 121 nodes on the surface.

3. Fine model:
   Finally, the whole area is subdivided into 25 blocks of 600 km $\times$ 600 km, respectively (Fig. 5.1c), resulting in 100 different models. Every block consists of 36 elements and has 49 nodes on the surface. This much finer resolution allows us to discuss results inside the ice-sheet shape and the regions beyond in more detail.

### 5.2.2 Ice load

The ice model for the Late Pleistocene glacial history in Europe is taken from the FBKS8 ice model of Lambeck et al. [1998a], and applied within the model area. The ice model FBKS8 simulates the extent and melting history of the Fennoscandian and Barents Sea Ice Sheets from the last glacial maximum (LGM) towards the present day. The extent of these ice sheets for four different epochs is shown in

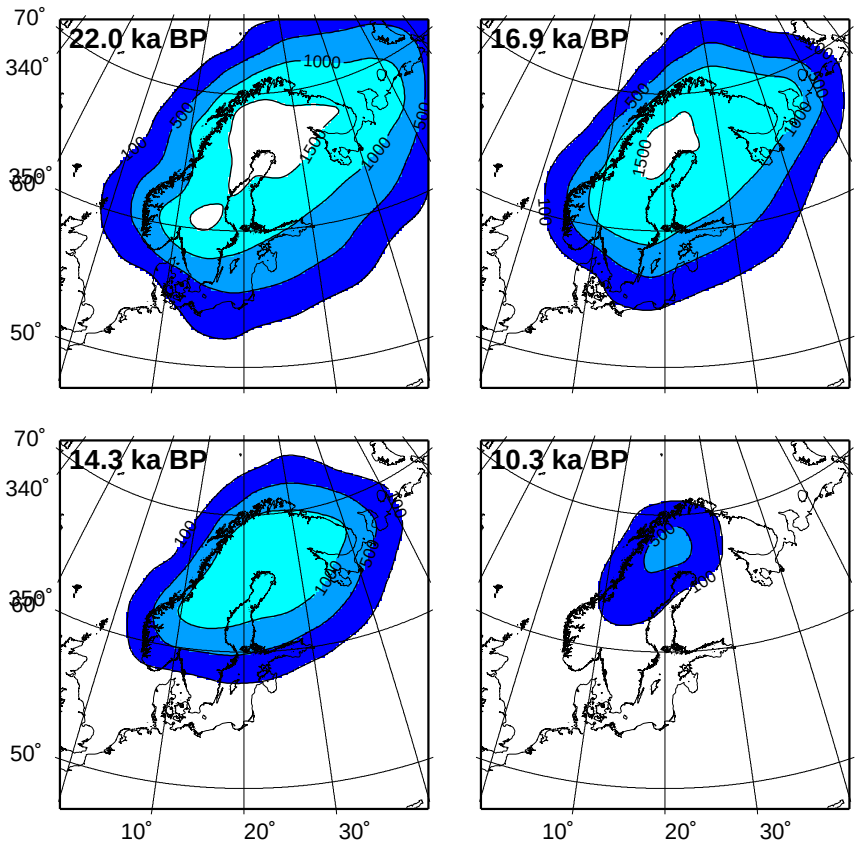


Figure 5.2: Map of ice model FBKS8 over Fennoscandia for four different time epochs. Contours are drawn every 500 m.

Fig. 5.2. The ice sheets are included in a high spatial and temporal resolution model that is consistent with the majority of the field evidence for ice-margin retreat and with the GIA data. The ice volume at the LGM approximately 22,000 years BP corresponds to 17 m of eustatic sea-level change. All reconstructions subsequent to the LGM are based on glaciological and geomorphological evidence and thus reflect the approximate extent of the Late Pleistocene ice sheets throughout the last glacial cycle. The time dependence of the load is applied as follows: A maximum load, corresponding to the LGM (at 22,000 years BP), is applied from 212,000 to 122,000 years BP. Then the load is instantly removed, and the model is ice free during the penultimate interglacial until 112,000 years BP. Then the load increases linearly, until it reaches its maximum extent at 22,000 years BP, followed by a detailed deglaciation history until the present. This parameterisation has been shown to be sufficient to correctly predict changes in surface displacements [Kaufmann et al., 2000; Kaufmann and Wu, 2002; Steffen et al., 2006a]. The ocean-load is not included, as the effects are at least one order of magnitude smaller than the ice-load signal [Steffen et al., 2006a].

## 5.3 Results

In this section we discuss and compare the modelling results of the different earth models, particularly the influence of certain regions to the BIFROST velocity predictions. The model predictions of present-day motions (uplift and horizontal movement) for the Scandinavian region are used to calculate the sensitivity kernels of a certain region. Furthermore, we discuss how selected stations of the BIFROST project [Johansson et al., 2002] are affected.

The calculation of the sensitivity kernels follows the approach given in Wu [2006], which is based on an expression given by Peltier [1998]. They are defined by:

$$K_{lj}(r) = K_{lj}(r_i) = \frac{\delta p_l}{\delta m_j(r_i)\,\Delta V_j(r_i)}. \tag{5.1}$$

$K_{lj}(r_i)$ is the sensitivity kernel with $l$ the location of the observation, and $j$ the number of the perturbed region (block number in Fig. 5.1). $r_i$ is the depth of the perturbed region, and thus $K_{lj}(r_i)$ corresponds to a certain model UM$i$_B$j$. In sections 5.3.1 to 5.3.3 of this paper, the location of the observation point $l$ is assumed to be directly above the location of the perturbed viscosity region. In section 5.3.4, we consider the effect of the block with viscosity change on crustal velocities measured in nearby blocks. The differential prediction $\delta p_l$ (in our case a horizontal velocity or uplift velocity) is defined as

$$\delta p_l = p_l^{3D} - p_l^{1D}, \tag{5.2}$$

with $\delta p_l^{3D}$ the prediction of a certain perturbed 3D model and $\delta p_l^{1D}$ the prediction of the 1D model V1 from Steffen et al. [2006a] (Fig. 5.3). $\Delta V_j$ is the fractional volume of the block $j$ in depth $i$:

$$\Delta V_j(r_i) = \frac{V_{ij}}{V_{model}}, \tag{5.3}$$

with $V_{ij}$ the block volume and $V_{model}$ the volume of the entire central area. The viscosity perturbation $\delta m_j$ of block $j$ in depth $i$ in our modelling is equal to 0.5, the difference of half an order of magnitude between the viscosities. The kernels are calculated for every surface grid point of the FE model and thus, we are able to make a sensitivity analysis for each location in the model area to the different blocks. However, this would produce a huge number of figures to show and interpret making the paper unreadable (Just

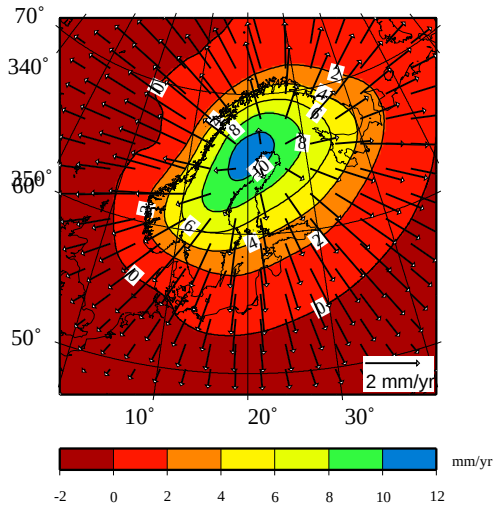


Figure 5.3: Predictions of horizontal (arrows) and vertical movement (contours) for the 1D model V1 from Steffen et al. [2006a].

take the 3 present-day velocity components at the 961 surface nodes with each of the nodes sensitive to a viscosity change in 4 depth ranges $i$ of the 25 blocks of the fine model. This would result in 72075 curves when drawn over the depth!). Hence, we introduce following approach: We calculate the kernel of a block UM$i$_B$j$, by averaging the perturbed predictions of all surface nodes of this block to one value for block UM$i$_B$j$. This means for the coarse and intermediate model averaging the values of 121 nodes to one value, and for the fine model averaging the values of 49 nodes to one value. With this approach an overview is given on how a viscosity change in a certain block influences on average the velocities at each surface point of the block area (Figs. 5.4 and 5.5). The effect of a block UM$i$_B$j_1$ at the locations of another block UM$i$_B$j_2$ is calculated by averaging all perturbed predictions of all surface nodes of block UM$i$_B$j_2$ to one value. Here, only selected examples are discussed as the number of curves is still large (Figs. 5.6 and 5.7). Finally, the results for the BIFROST stations discussed in Milne et al. [2004] are presented (Figs. 5.8 and 5.9). All these figures show the sensitivity kernels of the present-day velocities (in WE and NS–direction, and the uplift) over the depth as normalised Earth radius. They are interpreted as the sensitivity of one block or one BIFROST station to viscosity changes (i) in one of the 4 upper-mantle layers below that block area or station, or (ii) in one of the 4 upper-mantle layers next to that block area or station.

### 5.3.1 Coarse model (1000 km × 1000 km block models, central area)

Fig. 5.4 shows the sensitivity kernels of the velocities for 4 different 1000 km × 1000 km blocks of the coarse model. The present-day uplift velocity is most sensitive to the second and third layer, with a kernel amplitude of around 0.6 mm/yr in block B2. Except for B4, the first layer is also more sensitive than the fourth one. Furthermore, viscosity changes in blocks B1-B3 result in an additional uplift, while block B4 induces an additional subsidence component, when compared to the 1D viscosity model.

For the present-day horizontal velocity in WE–direction, we generally find a smaller kernel amplitude of around 0.1 mm/yr, and an increase in sensitivity to deeper parts of the upper mantle and/or only small variations in the first 3 layers. The blocks B1 and B3 west of the model centre show an additional

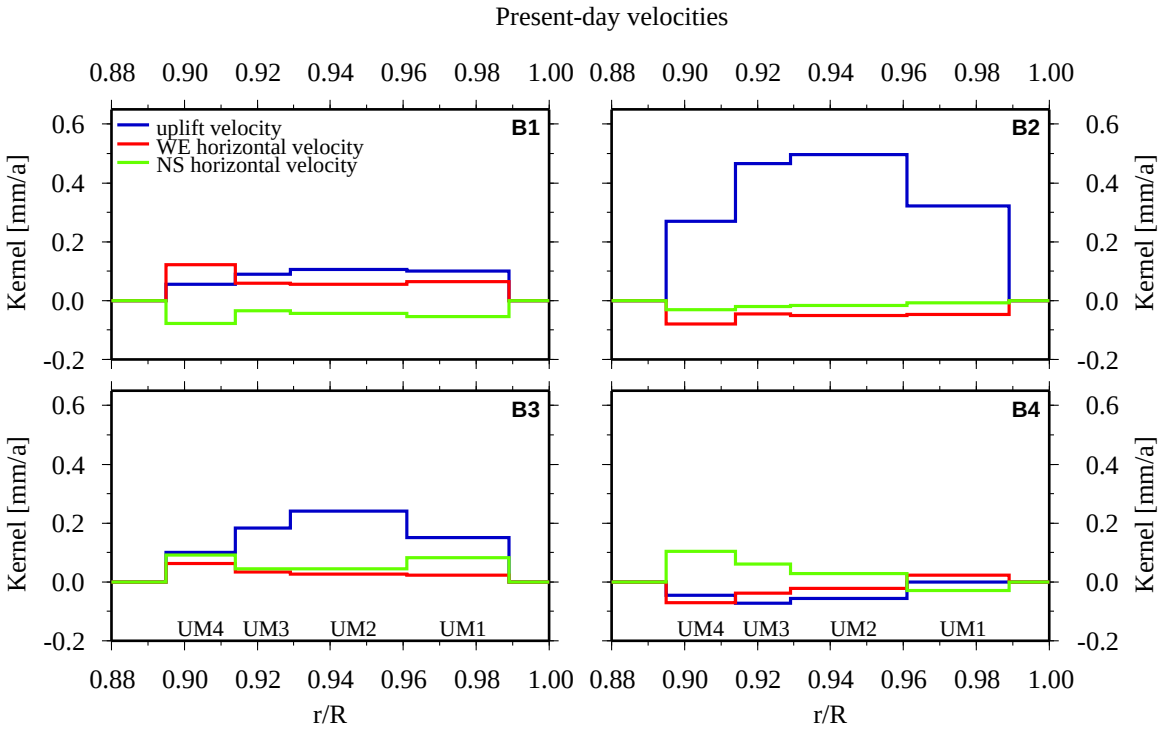


Figure 5.4: Sensitivity kernels of the present-day velocities plotted as a function of the normalised Earth radius for the coarse model.

movement to east, while the additional movement in blocks B2 and B4 east of the model centre is directed to west, except for the first upper-mantle layer in B4. Since the horizontal movement due to the uplift is generally directed outward, these differences in the horizontal velocity between the 1D model and the perturbed 3D model indicates that a higher viscosity in the perturbed region results in a decrease of the horizontal radially outward motion. For B1-B3, the sensitivity of the lowest part of the upper mantle is around twice that of the other parts. These blocks lie within the former ice sheet. In contrast to this, the sensitivity for B4, where most parts are located outside the former ice sheet, is small and directed eastward in the first layer. Also, the sensitivity changes sign but increases in magnitude at the deeper part of the upper mantle. For B1, which is located in the northwestern part of the former ice sheet and in the region with the highest amount of ice, the largest sensitivity with around 0.13 mm/yr is obtained.

The sensitivity of the present-day velocity in NS–direction, with a kernel amplitude of around 0.1 mm/yr, shows again the highest sensitivity at the bottom of the upper mantle, except for the first upper-mantle layer beneath B3. Here, compared to the sensitivity in the fourth layer the sensitivity is relatively higher. Besides this, an additional northward directed motion is found for blocks B3 and B4, which are located in the south of the model, and the additional southward motion for the two blocks B1 and B2, that are located in the northern part. This confirms again the decrease of the horizontal velocities due to the higher viscosity of the perturbed region. In summary, comparison of the tangential motion of our four models with the results of the 1D model shows that a lateral viscosity variation in the transition zone has a strong influence on the tangential motion.

The results of this section have many similarities with the next two sections. Thus, we first state and summarise the common findings in the next sections and then discuss differences.

### 5.3.2 Intermediate model (1000 km × 1000 km block models, whole area)

In Fig. 5.5 the sensitivity of the present-day uplift velocity can be seen for the nine blocks with a maximum kernel amplitude of around 0.6 mm/yr at most. Generally, the kernels are positive within the ice margin and negative outside. As expected, the largest effects are found for B5, the block above which the former ice maximum was located. The uplift velocity is most sensitive to the second and third upper-mantle layer. The effect from the fourth layer reaches only around 60% of the second layer and is smaller than the one of the sub-lithospheric layer. The sensitivity of variations in other blocks is smaller with the smallest sensitivities for B4 and B6.

The sensitivity kernels of the present-day horizontal velocity in WE–direction shows kernel amplitudes of around 0.2 mm/yr. The first diagram row encompasses the northern model parts. As for the coarse

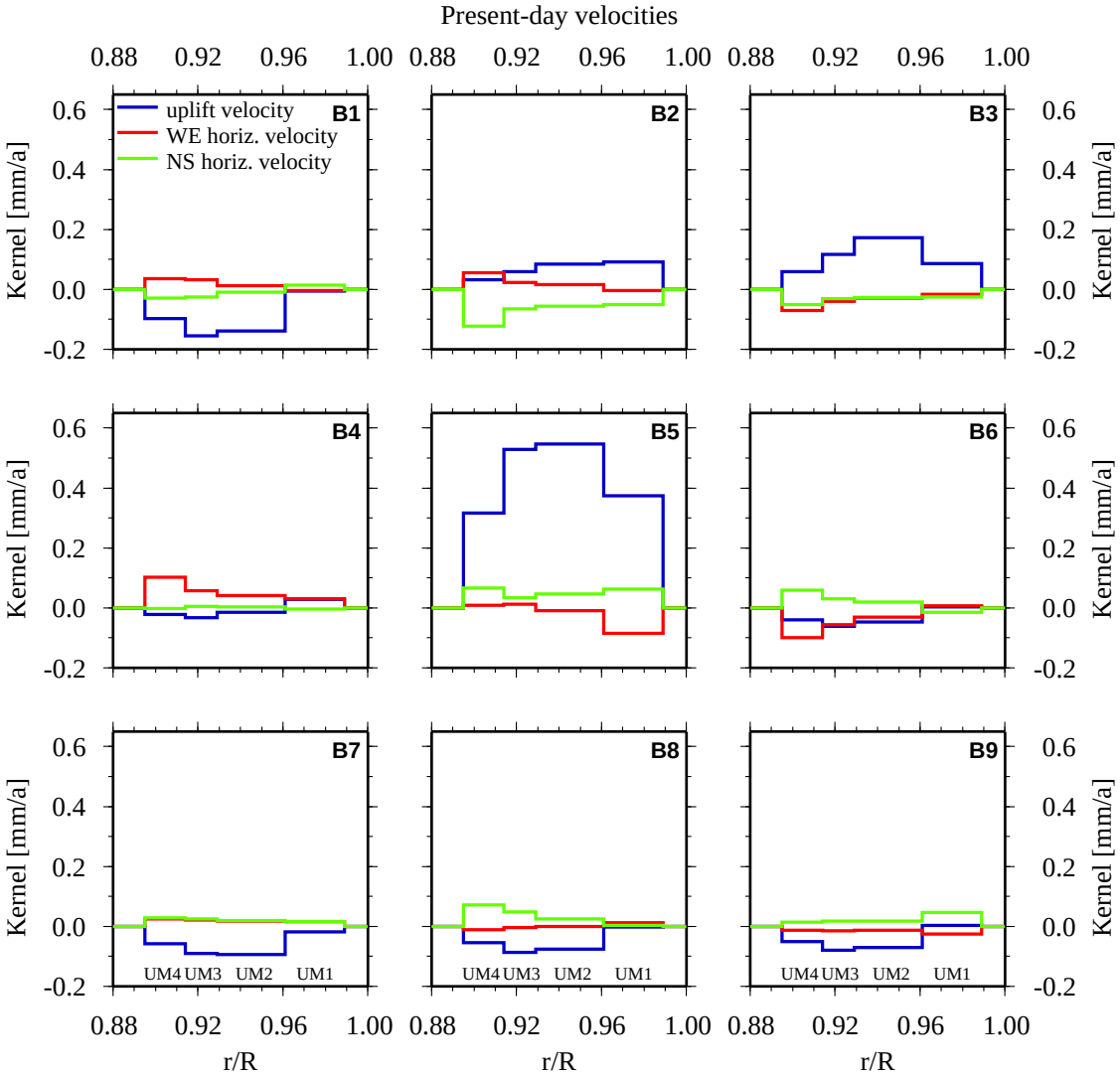


Figure 5.5: Sensitivity kernels of the present-day velocities plotted as a function of the normalised Earth radius for the intermediate model..

model (section 5.3.1), we also find that the higher viscosity reduces the outward directed horizontal motion from the centre of rebound. For B1 the kernel has nearly the same sensitivity in the transition zone (third and fourth layer), while for the first layer it is negligible. For B2 we observe an eastward trend, which indicates a decrease of the uplift-induced westward movement due to the higher viscosity in the perturbed region. The ice sheet was located on top of B2 and also B3, east of B2. The surface was depressed mainly in those two regions of the northern parts, which after the disappearance of the ice mass now induces westward directed velocities on B2 and eastward directed velocities on B3. The second diagram row summarises the results of central model blocks B4 to B6. For B4 and B6 comparable results to B1 and B3 can be established, except that B4 has larger kernels than B1 due to the thicker ice load on top of B4's surface. The most impressive behaviour is found for B5. Here, the WE–velocity is most sensitive to the first upper-mantle layer. This is a consequence of the ice load, which was largest on B5's surface among all other blocks (see Fig. 5.1) and acts directly in the uppermost mantle parts and hence, for the WE–velocity in the first layer. The last diagram row highlights the sensitivity for B7 to B9. As there is only a small surface load we find only small sensitivities. For B7 and B8 the sensitivity in the fourth layer is still the largest. For B9 the first layer is the most sensitive, which is the block with the smallest surface load of all 9 blocks.

Fig. 5.5 also summarises the sensitivity of the present-day horizontal velocity in NS–direction for the nine blocks. For the northern blocks of the model, we can confirm the highest sensitivity of the fourth layer to NS–velocity and the southward movement due to the viscosity contrast between the underlying block and the rest of the blocks in a specific layer. The second diagram row focuses on the central model area. Interestingly, B4 is nearly insensitive to the NS–velocity, as here horizontal velocities are mainly in the western direction. For B5 a high sensitivity can be found in all layers, with maxima in the first and fourth layer. This is, as already mentioned in the discussion of the WE–velocity, a consequence of the large ice load on the surface of this block. B6 is again most sensitive to the lowest part of the upper mantle, indicating a northward motion, which is due to the ice load on B3 to the north. The sensitivity of B7 and B8 is highest in the fourth layer, but for B7 smaller than for B8. In contrast to this, B9 shows the highest sensitivity in the first layer. The movement to north for the last three blocks is due to the viscosity contrast.

### 5.3.3 Fine model (600 km $\times$ 600 km block models)

We do not show here the results of the fine model, as they are comparable to the former results. A rough comparison of the results of smaller and bigger blocks indicates higher sensitivities for the horizontal velocities of bigger blocks. In contrast, the uplift velocity of smaller blocks has a higher sensitivity than that of the bigger blocks. Thus, we clearly see a dependence of the sensitivity kernels on the size of a block. This means if we scale down the block size, the sensitivity to uplift velocity would increase and the horizontal velocity would decrease. In addition, both grids show that blocks within the former ice sheet are more sensitive than blocks beyond. The biggest values are obtained for blocks in the former ice sheet centre with the maximum ice height.

### 5.3.4 Sensitivity of blocks in selected distances

The results shown in the previous sections focus on the sensitivity of a disturbed block on the averaged crustal motion directly above the block itself. In this section we investigate the influence of viscosity changes in a selected block to the locations on surrounding blocks. However, we only focus on the

present-day horizontal velocities, because the effect on the uplift velocity of a neighbouring block of a perturbed block is negligible. Hence, we do not show any figure for this case.

Fig. 5.6 summarises the sensitivity kernels of three blocks of the coarse model (Fig. 5.1a) to the neighbouring blocks for the present-day horizontal velocities. We observe again the biggest sensitivities in the first and the fourth upper-mantle layer, but a discussion of the effects is quite complicated. Generally, the horizontal velocities in each block are mainly influenced by viscosity changes in blocks 2 and 3, which have the thickest ice. For example, Fig. 5.6d and h show that both velocities at B4 are most sensitive to viscosity changes in the third and fourth layer of B3, and also to the first and second layer of B2. The velocities at B3 are mainly influenced by B2, while velocities at B2 are most sensitive to B3 in NS–direction and to B1 in WE–direction. At B1 the NS–velocity shows the biggest sensitivity to B3. For the WE–velocity contributions by all other blocks are observed.

Fig. 5.7 shows the sensitivity kernels for the intermediate model, in one case for block B5 to the 8 other blocks (Fig. 5.7a, b, e and f), and in the other case each of these 8 blocks to B5 for the present-day horizontal velocities (Fig. 5.7c, d, g and h). Fig. 5.7a and b highlights a strong influence of viscosity changes in the first layers of B5 on the present-day WE velocity at the other surrounding blocks, which tends to decrease with deeper upper-mantle layers. The same behaviour is observed for block B5 on blocks B1 to B9 for the NS–velocity (Fig. 5.7e and f). The influence of block B5 on B3 and B4 is small on the NS–velocity, while the influence on the NS–velocity at B2 shows maxima in the first and fourth layer. The influence of viscosity changes in the 8 other blocks on WE–velocity at B5 (Fig. 5.7c and d) is twofold: on the one hand, the sensitivity due to changes in B1, B2 and B7 to B9 is low and / or decreases towards the deeper parts of the lower upper mantle, on the other hand, changes in each upper-mantle layer of B3, B4 and B6 show a nearly constant influence on WE–velocity at B5. Interestingly, these are three blocks with a thick ice cover. Furthermore, B4 and B6 are situated west and east of B5, respectively, in the same direction as the discussed velocity component. Fig. 5.7g and h reveals comparable effects. Here, B2, B8 and B3 show a constant influence, while the sensitivity for NS-velocity generally decreases with deeper depth as in WE-velocity. Again, B2 and B8 are located in the direction of the resulting velocity component, north and south of B5.

The comparison, in view of the grid size, indicates similar behaviour between the intermediate model and the fine model. Two main results arise: (i) the influence of a perturbed block on the uplift velocity of a neighbouring block is negligible (not shown), and (ii) the influence of one block on the horizontal velocity on another block is strongest if the direction of the horizontal velocity is along the same direction between the two blocks. In the case of a block located right next to the perturbed block, the other component is much less affected. Additionally, the amplitude of the sensitivity kernel decreases as the distance between the two blocks increases.

### 5.3.5 Effects on BIFROST stations

Figs. 5.8 and 5.9 show the sensitivity kernels of the present-day velocities for 8 selected BIFROST stations due to viscosity changes directly below the block. These 8 stations are the same as those taken by Milne et al. [2004], oriented along a North-South-profile. The locations can be found in Fig. 5.1.

*Coarse model:*
Fig. 5.8 focuses on the results for the coarse model. The sensitivity in the uplift velocity generally increases for the central BIFROST locations, with the lowest sensitivity found for the stations Hässleholm and Kevo in the far south and north. Looking at the sensitivity to the upper-mantle layers, the maximum is resolved for the second and third layer. At Sundsvall, Skelletea and Sodankyla the sensitivity in the

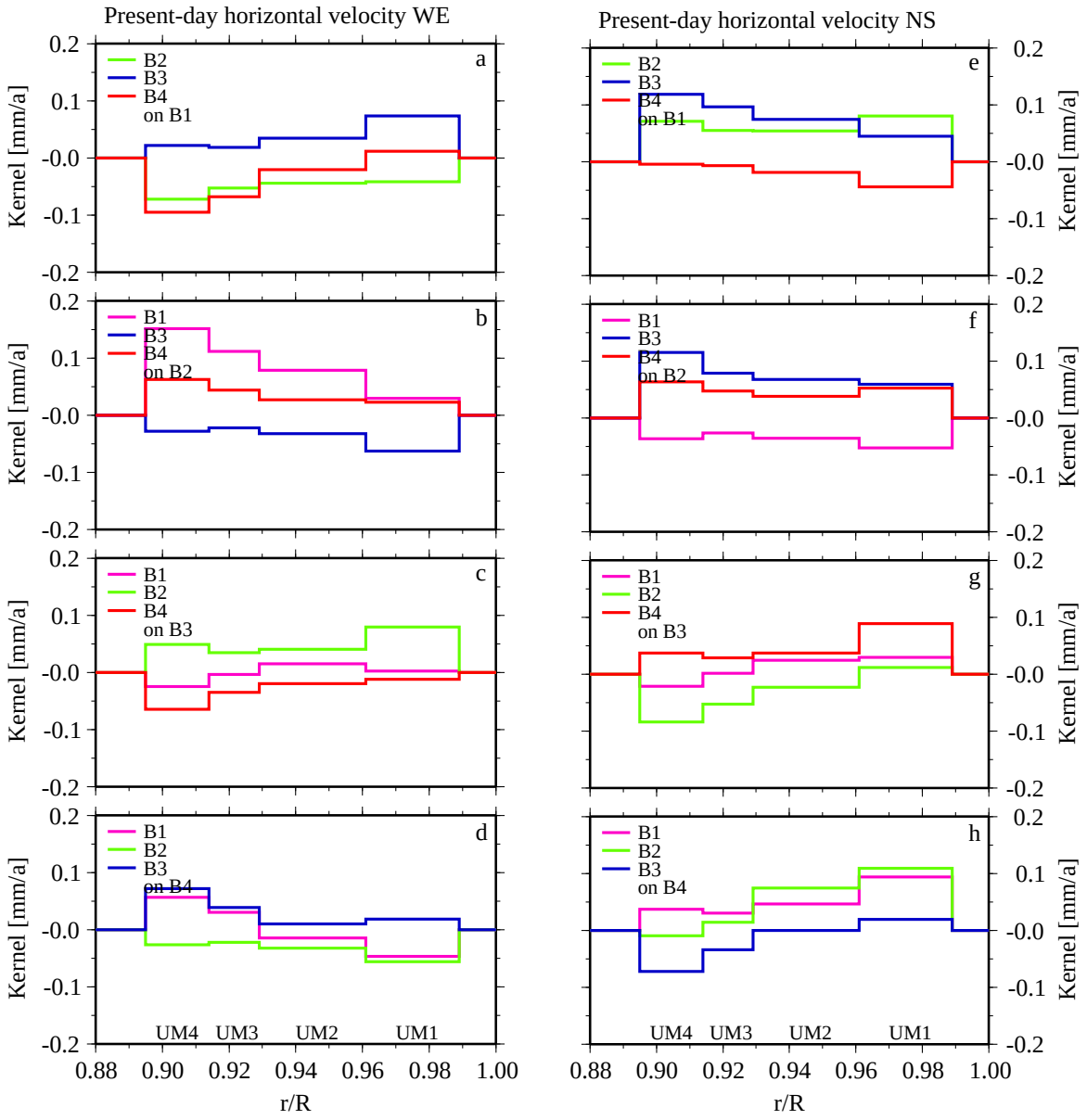


Figure 5.6: a - d) Sensitivity kernels for the coarse model of three out of four blocks on the fourth one for the present-day horizontal velocity in WE–direction plotted as a function of the normalised Earth radius. e - h) Same as a and b, but for the present-day horizontal velocity in NS–direction.

third layer is slightly larger than in the second layer. The first layer is, except for the three central stations Martsbo, Sundsvall and Skelletea, more sensitive than the fourth layer. The sensitivity of the horizontal velocities is different, when compared to the results averaged for one block (Figs. 5.4 - 5.7), as the general tendency to increase in the deeper upper mantle is only partially observed (WE–horizontal velocity at Hässleholm, Jonkoping, Sodankyla and Kevo). Instead, the second and third upper-mantle layer often dominate the sensitivity. In exception, the NS–horizontal velocity at Hässleholm, Jonkoping and Norrkoping is characterised being most sensitive to the first and fourth layer with slightly higher values in the fourth layer. At Martsbo, this component shows a nearly constant sensitivity to all layers.

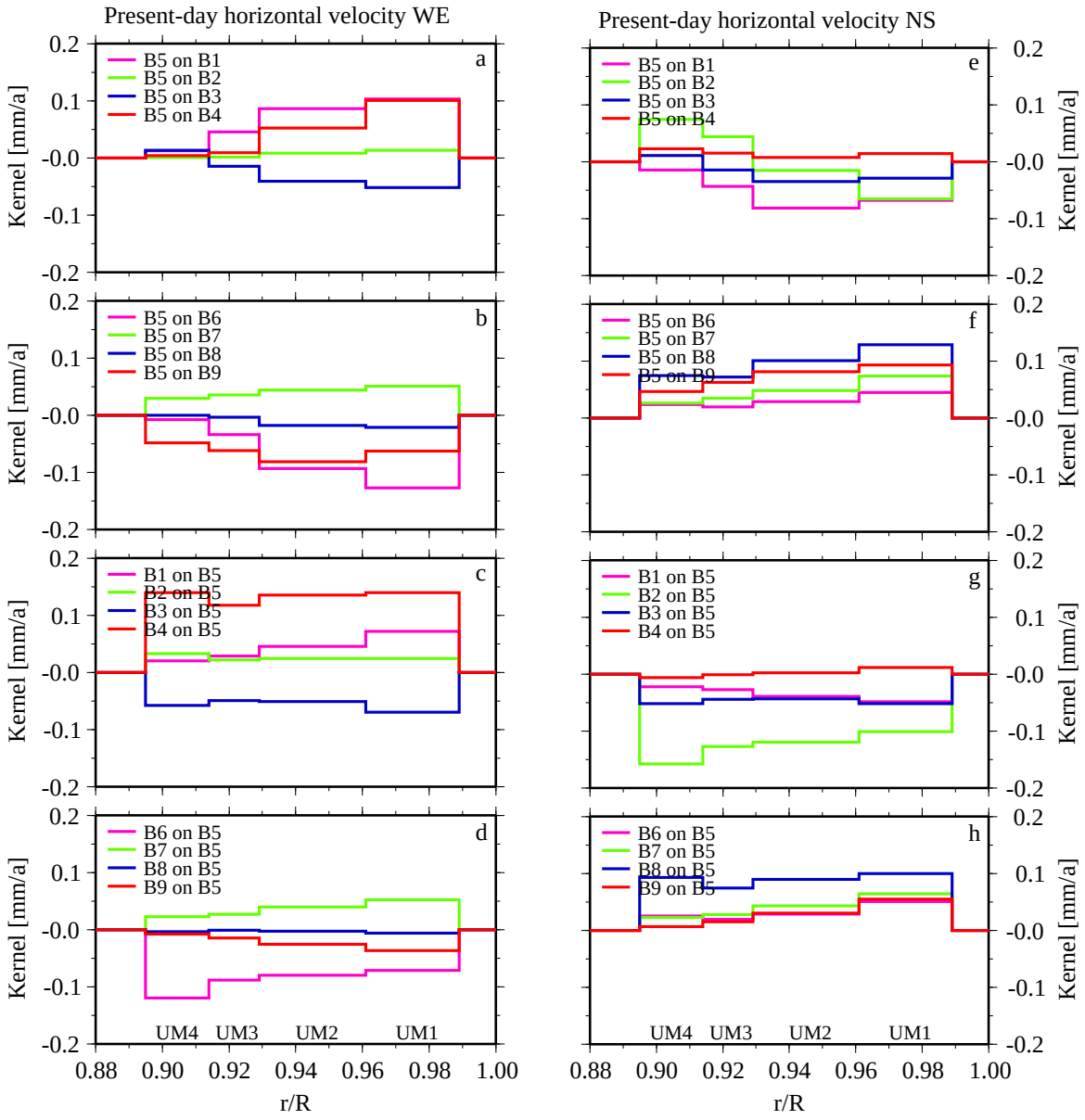


Figure 5.7: a and b) Sensitivity kernels of the central block B5 of the intermediate model on the eight other blocks for the present-day horizontal velocity in WE–direction plotted as a function of the normalised Earth radius. c and d) Sensitivity kernels of the eight outer blocks of the intermediate model on block B5 for the present-day horizontal velocity in WE–direction plotted as a function of the normalised Earth radius. e and f) Same as a and b, but for the present-day horizontal velocity in NS–direction. g and h) Same as c and d, but for the present-day horizontal velocity in NS–direction.

*Intermediate model:*

Fig. 5.9 is the same as Fig. 5.8, but for the intermediate model. As for the coarse model, the uplift velocity (i) is most sensitive in the second and third layer and (ii) reaches its largest values at the central BIFROST stations. At Sundsvall and Skelletea the third layer is the most sensitive. Furthermore, at these two stations the fourth layer is more sensitive than the first layer. Interestingly, those stations are located

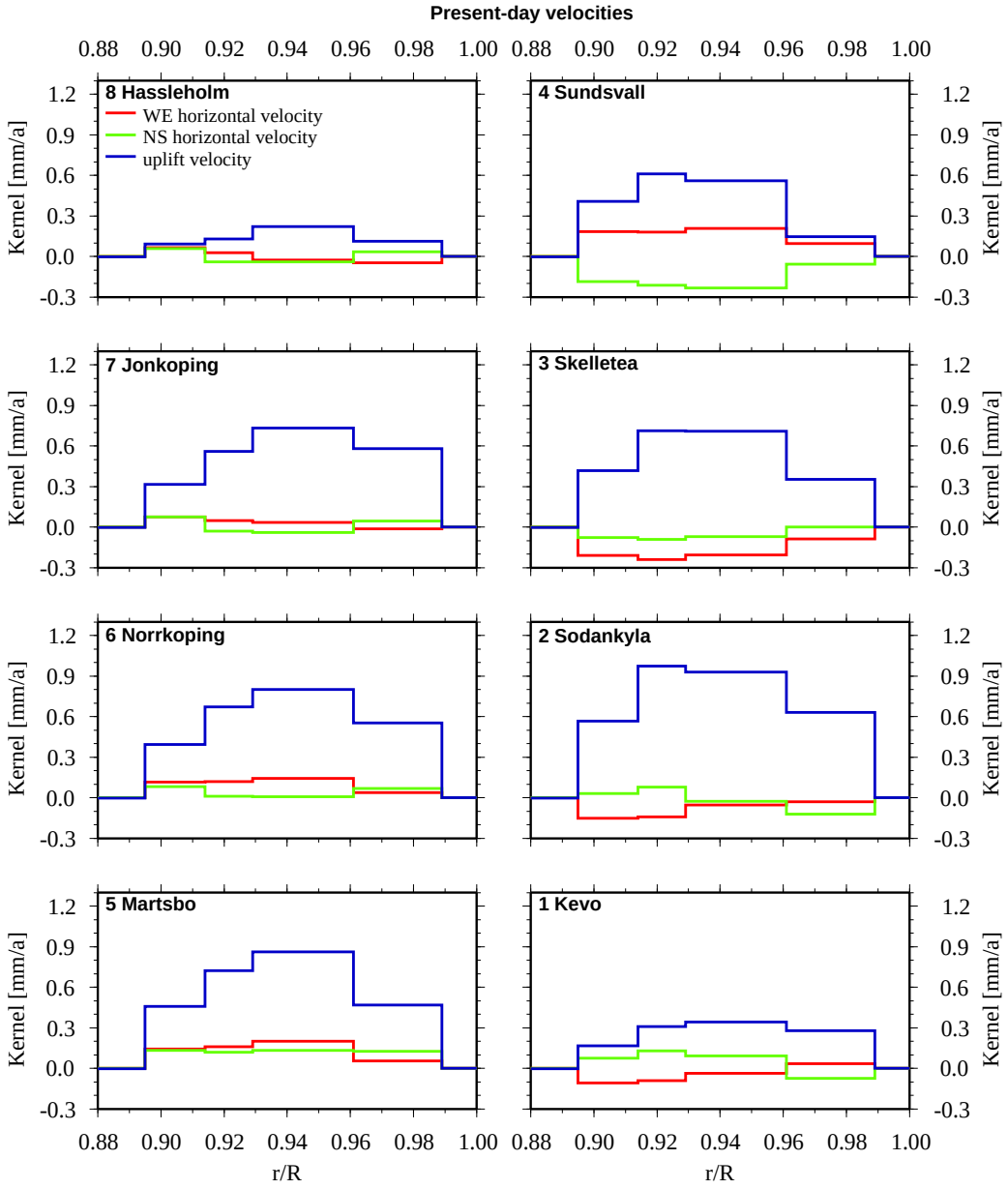


Figure 5.8: Sensitivity kernels of the present-day velocities of 8 BIFROST stations for the coarse model plotted as a function of the normalised Earth radius.

in the centre of the former ice sheet and are also the ones where Milne et al. [2004] found the largest sensitivities. The station of Jonkoping seems to be insensitive to variations in the fourth upper-mantle layer. The horizontal velocities are influenced differently. For example, at Hässleholm the sensitivity is low, but with a maximum in the fourth layer. At Sodankyla, the WE–velocity is most sensitive from the second to the fourth layer, but negligible in the first layer, while the sensitivity of the NS–velocity remains quite constant in all layers. At Jonkoping, Norrkoping and Martsbo a decrease in sensitivity to deeper parts is observed, while at Kevo an increasing trend results.

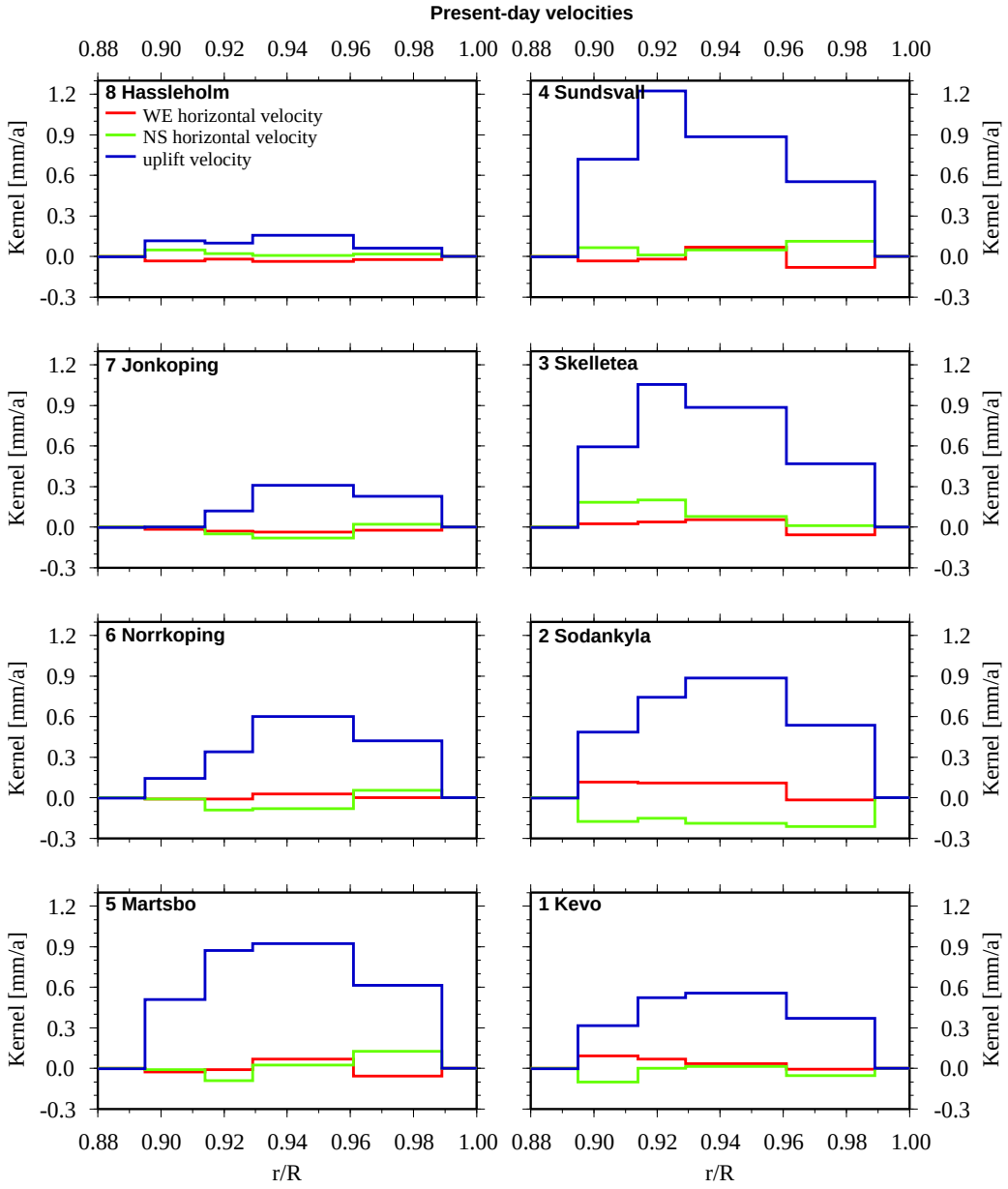


Figure 5.9: Sensitivity kernels of the present-day velocities of 8 BIFROST stations for the intermediate model plotted as a function of the normalised Earth radius.

In agreement with the results of Milne et al. [2004] and independent of the block size, the uplift velocity obtained with the different block grids also shows the largest sensitivity values at the stations of Sundsvall and Skelletea, followed by Martsbo and Sodankyla, then Norrkoping, Jonkoping and Kevo, and finally the smallest values are found at Hässleholm. In contrast, the difference between the third and fourth layer is greater than between a (simply resolved by averaging the respective layers) third and fourth layer of Milne et al. [2004]. For the horizontal velocities a different behaviour is established, which we think is mainly due to the model geometry and thus due to the “simple” lateral heterogeneity of our 3D model. Our results do not show the decrease in sensitivity of horizontal velocities to deeper upper-mantle parts

(except for the NS–velocity at Skelletea and Sodankyla) as observed by Milne et al. [2004]. They are more affected by the location of a station on a block in relation to the location of the block in the model, the distance of the station to the block border and the ice sheet geometry, which finally confirms the results of Wu [2006]. This effect can be seen with a closer look at the results. If we take for example the station of Hässleholm, it is located on the 4 block model in the centre of B3. The uplift velocity is small compared to other stations due to the smaller ice load. The direction of the horizontal velocities in each layer differs due to the location in the centre. This becomes clearer when looking at Hässleholm and its location on the 9 block model. Here, Hässleholm is situated in the northwestern corner of B8. The uplift velocity is, as expected, still small, but the horizontal velocities clearly show a movement to west for the WE–component and north for the NS–component. These analyses can be done for each of the 8 BIFROST stations and their position on the different block models. The results confirm the behaviour discussed above.

*Fine model:*
Fig. 5.10 shows the sensitivity kernels for the BIFROST stations of Norrkoping, Sundsvall and Kevo and the perturbed blocks B13 to B53 of the fine model (see Fig. 5.1c). Thus, this figure summarises on a block profile from north to south the influence of a viscosity change on the present-day velocities of the three stations. The station of Norrkoping is located in the northwestern part of block B43. Hence, the largest effects on this site in Fig. 9 are due to this block. Remarkable effects are also found for the uplift velocity for a perturbed block B33. This is due to the location of Norrkoping on block B43 next to block B33, which in addition is located in the centre of the Fennoscandian ice sheet. Again, the largest effects are found in the second layer. The sensitivity of the horizontal velocity is smaller but not negligible. The contributions of the other blocks (B13, B23 and B53) are small and they decrease more as the region of viscosity change gets further away. As shown here, the amplitude of the uplift velocity decreases much faster than that for the horizontal velocities. The station Sundsvall is located near the middle of block B33, which is reflected by the amplitude of the kernels. The uplift velocity is largest at B33 and strongly decreases as the viscosity change moves farther away. Interestingly, the largest amplitude in the uplift kernel in B23 and B43 is found in the fourth layer, while the sensitivity in the second layer is very small. The horizontal velocities show a different behaviour. The amplitude of the NS-velocity kernel first increases in the nearby blocks B23 and B43, then it decreases with increasing distance, while the WE-velocity steadily decreases. This behaviour is due to the location of the perturbed block and the direction of the component. The opposite is observed for a WE block profile (not shown). The results for Kevo have many similarities with the one for Norrkoping, as Kevo is located quite near the block border to B13. As expected, due to its close proximity, the influence of the neighbouring block B13 on uplift velocity is comparable to that for B23. The exception is in the fourth layer where the amplitude due to viscosity change in B13 is larger by a factor of 10.

These results can be summarised as follows: (i) for a selected station, the sensitivity of the uplift velocity is largest for the block where the station is located and may include the neighboring block, if the station is located close to its border, (ii) the sensitivity of the uplift velocity strongly decreases as the viscosity change moves farther away, (iii) the sensitivity for the horizontal velocity component is largest at the neighbouring block if that block is situated in the direction of this component, (iv) the sensitivity of the horizontal velocities increases at the neighbouring block but decreases as one moves further away, (v) the amplitude of the uplift velocity decreases much faster with distance than that for the horizontal velocities.

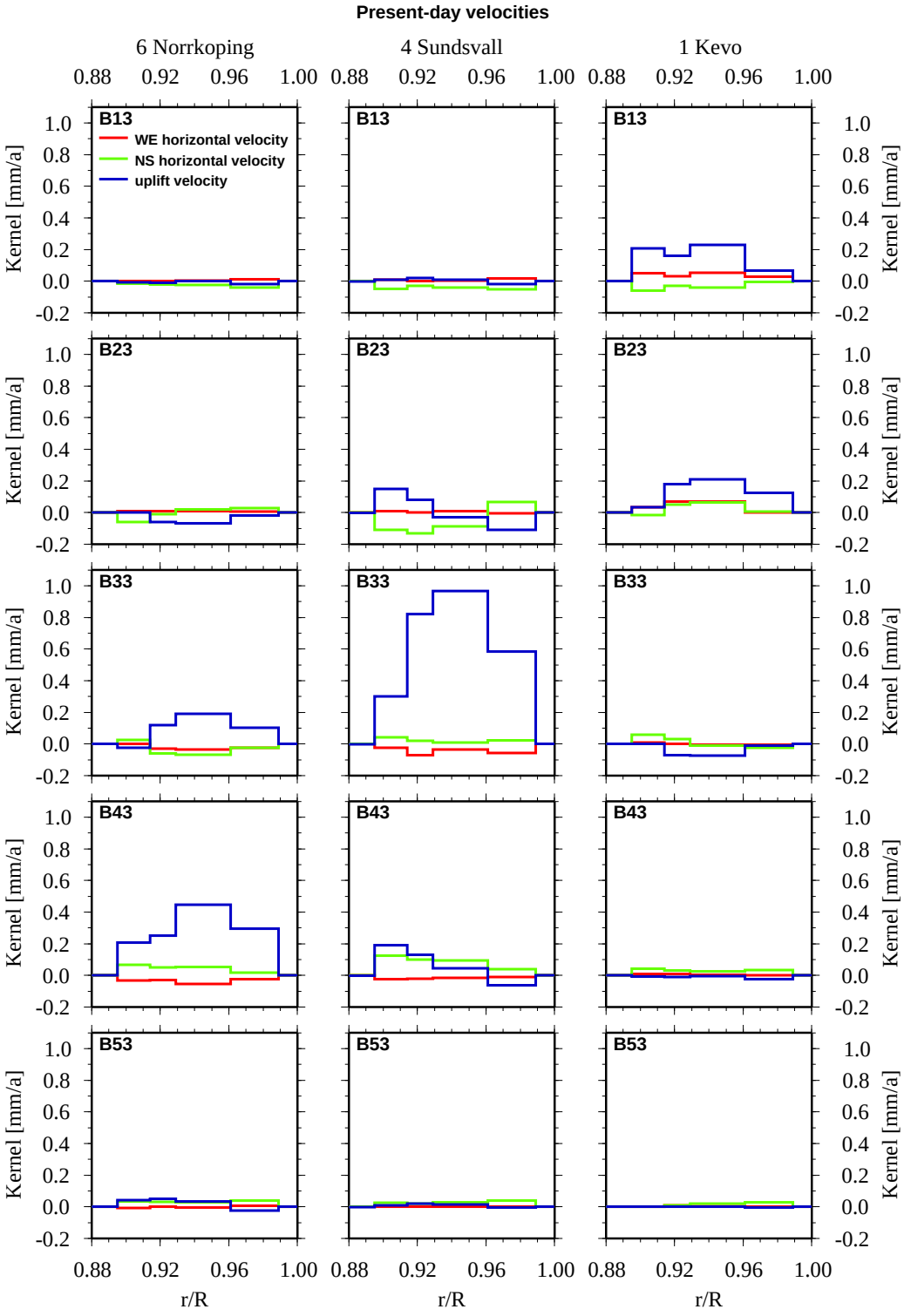


Figure 5.10: Sensitivity kernels of the present-day velocities at 3 BIFROST stations and 5 selected 600 km × 600 km blocks plotted as a function of the normalised Earth radius.

## 5.4 Conclusions

We have investigated the sensitivity kernels of the present-day velocities in Fennoscandia with a 3D FE model with compressible, viscoelastic material properties and a realistic ice-load history of the Fennoscandian ice sheet, which allowed us to explore the sensitivity of different data from different parts of Fennoscandia. Therefore, we have subdivided the model into different blocks and have changed the viscosity in a certain block by half an order of magnitude as suggested by Wu [2006]. The different subdivisions yielded in a huge number of kernels to interpret and thus we have introduced an approach to calculate the kernel of a block by averaging the perturbed predictions of all surface nodes of this block to one value for this block.

Our results show that the present-day uplift velocity is most sensitive to the second and third layer of the upper mantle independent of the block size and the sensitivity for the second layer is generally higher than that in the third one. This is in agreement with the findings from Steffen et al. [2006a], who observed in their simple sensitivity analysis high contributions to uplift velocity from those two layers. The first layer is also more sensitive than the fourth one. Furthermore, viscosity changes in blocks within the former ice sheet produce larger effects than blocks with mainly parts outside the former ice sheet. The largest effects are found for blocks located below the former ice maximum. The effect of a viscosity change in neighbouring blocks to one block on the uplift rate is negligible. The uplift velocity of smaller blocks is more sensitive than the one of bigger blocks. For the smaller blocks is also observed, that the sensitivity in the surrounding blocks of the maximum sensitivity decreases up to the minimum for blocks far away of the shape of former ice sheet. Thus, we see a clear influence of the block size on our results.

For the present-day horizontal velocity and bigger blocks, we generally found an increase in sensitivity to deeper parts of the upper mantle and/or only small variations in the first 3 layers. In contrast, the first upper-mantle layer is most sensitive for the smaller blocks. The smallest influence is obtained for the second layer. Deeper into upper mantle, the sensitivity increases. For all block sizes we establish the directed movement of the kernels out of the perturbed block induced by the higher viscosity in that block. For blocks within the former ice sheet, the sensitivity in the lowest part of the upper mantle is around twice as much as the sensitivity of the other parts. In contrast, the sensitivity at the block below the former ice sheet maximum is most sensitive to the first layer. The sensitivity for blocks with most parts located outside the former ice sheet is small. In summary, comparison of the horizontal motion of the perturbed models with the results of the 1D model shows that a lateral viscosity variation in the transition zone has a strong influence on the horizontal velocities. A comparison of the results of smaller and larger blocks also indicates higher sensitivities for the horizontal velocities of larger blocks.

The sensitivity of a selected block to the surrounding blocks is for the horizontal velocities large in the first and the fourth upper-mantle layer. It is mainly influenced by viscosity changes in blocks with ice load on the surface. The strongest influence results from blocks which are located in the direction of the discussed horizontal component. For the smaller blocks, different results are obtained, which makes it quite complicated to analyse. The uplift velocity is less influenced at all blocks.

The sensitivity kernels of the present-day velocities for 8 selected BIFROST stations represent in the uplift velocity generally an increase in sensitivity for the central BIFROST locations. The lowest sensitivity is found for the stations in the far north and south. The maximum is resolved for the second and third layer and the first layer is generally more sensitive than the fourth layer. This confirms the results for the blocks except for a few sites near the load centre. The sensitivity of the horizontal velocities is not comparable with the results for the blocks, as the second and third upper-mantle layer also can dominate the sensitivity. This is in agreement with the results of Milne et al. [2004]. In contrast, the difference

between the third and fourth layer is greater. The horizontal velocities are more affected by the location of a station on a block in relation to the location of the block in the model, the distance of the station to the block border and the ice sheet geometry, which confirms the results of Wu [2006].

In view of the ideal location of GPS stations in Fennoscandia to determine the viscosity structure beneath we would like to point out:
(i) Steffen et al. [2006a] showed that GPS data from Fennoscandia include less information of the lower-mantle viscosity, and thus it is not possible to resolve a sufficient heterogeneous structure. Nevertheless, a detailed picture of the upper-mantle viscosity can be obtained with a net of stations located in the shape of the former ice sheet.
(ii) The stations far outside the former ice sheet shape contribute to the determination of lateral viscosity contrasts in the upper mantle beneath Fennoscandia. As this is dependent on the size of a perturbed region and the location of this region to the GPS station, further investigations have to be made with a preliminary, but reliable viscosity structure of Fennoscandia.

## Acknowledgements

Many thanks to Kurt Lambeck for providing the FBKS8 ice model. The figures in this paper are drawn using the GMT graphics package Wessel and Smith [1991, 1998]. This research was funded by the DFG (research grant KA1723-1).